Chem. Mater. **2000,** *12,* 495−500 495

Zero Band-Gap Polymers: Quantum-Chemical Study of Electronic Structures of Degenerate π-Conjugated Systems

Sung Y. Hong*

Department of Chemistry, Institute of Natural Science, Kosin University,
Pusan 606-701, South Korea

Received August 23, 1999. Revised Manuscript Received December 13, 1999

In search of very small band-gap polymers, we have quantum-chemically investigated the electronic structures of various polypentafulvalenes (PFVs) fused with six-membered rings. Geometrical parameters of the polymers were optimized through semiempirical Hartree−Fock band calculations at the Austin Model 1 (AM1) level. Electronic structures of the polymers were obtained through modified extended Hückel band calculations by adopting AM1-optimized geometries. It is predicted that poly(di-vinylenedioxy-pentafulvalene) and poly(di-vinylenedithia-pentafulvalene) would possess nearly zero band gaps (corresponding to λ_{max}) despite their large bond-length alternation of $\sim$0.1 Å. However, these polymers are expected to be very susceptible to oxidation. Poly(di-2-butenylene-pentafulvalene) and poly(dipyrazinopentafulvalene) are estimated to possess band gaps comparable with that (1.13 eV) of PFV. The calculated band gap of poly(di-ethylenedioxy-pentafulvalene) is 0.77 eV, smaller than that of PFV by 0.36 eV. We explained the evolution of the band gaps of the polymers through molecular orbital arguments.

Introduction

In the mid-1970s poly(sulfur nitride), $(SN)_x$, was discovered to exhibit metallic character[1] and superconducting properties.[2] Since then a great deal of experimental and theoretical efforts have been devoted to searching for new conducting organic polymers, and as a result, a variety of conjugated polymers have been reported to be capable of achieving metallic conductivity upon doping with electron donors or acceptors.[3−7] During the past decade these efforts on conducting organic polymers have mainly been focused on structural modification of heterocyclic polymers for designing very small band-gap polymers[8−16] since Brédas demonstrated that the band gap of an aromatic system decreases as quinonoid character of the backbone increases.[17] However, the demonstration of Brédas is true only if the aromatic form is more stable in the ground state than the quinonoid form. In fact, it has been revealed that the more stable isomer (either an aromatic or a quinonoid form) possesses the larger band gap.[18−23] Therefore, the transition between two nondegenerate structures, aromatic and quinonoid forms, leads to a difficulty in designing a small band-gap polymer in the ground state. Our previous analysis indicated that the band gap (defined as the λ_{max} value) of a nondegenerate system in the ground state could rarely be achieved below 1 eV due to the transition between the isomers.[24] To our knowledge, among experimentally prepared polymers

---

* E-mail: shong@sdg.kosin.ac.kr. Fax: +82 51 405 9760.

(1) Walatka, V. V., Jr.; Labes, M. M.; Perlstein, J. H. *Phys. Rev. Lett.* **1973**, *31*, 1139.

(2) Greene, R. L.; Street, G. B.; Suter, J. L. *Phys. Rev. Lett.* **1975**, *34*, 577.

(3) Shirakawa, H.; Louis, E. J.; MacDiarmid, A. G.; Ching, C. K.; Heeger, A. J. *J. Chem. Soc. Chem. Commun.* **1977**, 578.

(4) Ivory, D. M.; Miller, G. G.; Sowa, J. M.; Shacklette, L. W.; Chance, R. R.; Baughman, R. H. *J. Chem. Phys.* **1979**, *71*, 1506.

(5) Rabolt, J. F.; Clarke, T. C.; Kanazawa, K. K.; Reynolds, J. R.; Street, G. B. *J. Chem. Soc., Chem. Commun.* **1980**, 347. Chance, R. R.; Shacklette, L. W.; Miller, G. G.; Ivory, D. M.; Sowa, J. M.; Elsenbaumer, R. L.; Baughman, R. H. *J. Chem. Soc., Chem. Commun.* **1980**, 348.

(6) Kanazawa, K. K.; Diaz, A. F.; Geiss, R. H.; Gill, W. D.; Kwak, J. F.; Logan, J. A.; Rabolt, J. F.; Street, G. B. *J. Chem. Soc., Chem. Commun.* **1979**, 854.

(7) Tourillon, G.; Garnier, F. *J. Electroanal. Chem. Interfacial Electrochem.* **1982**, *135*, 173. Yamamoto, T.; Sanechika, K.; Yamamoto, A. *J. Polym. Sci., Polym. Lett. Ed.* **1980**, *18*, 9. Lin, J. W. P.; Dudek, L. P. *J. Polym. Sci., Polym. Lett. Ed.* **1980**, *18*, 2869.

(8) Kobayashi, M.; Colaneri, N.; Boysel, M.; Wudl, F.; Heeger, A. J. *J. Chem. Phys.* **1985**, *82*, 5717.

(9) Jenekhe, S. A. *Nature* **1986**, *322*, 345.

(10) Bräunling, H.; Blöchl, G.; Becker, R. *Synth. Met.* **1991**, *41*−*43*, 487.

(11) Bräunling, H.; Blöchl, G.; Becker, R. *Synth. Met.* **1991**, *41*−*43*, 1539.

(12) Hanack, M.; Mangold, K.-M.; Röhrig, U.; Maichle-Mössmer, C. *Synth. Met.* **1993**, *60*, 199.

(13) Lorcy, D.; Cava, M. P. *Adv. Mater.* **1992**, *4*, 562.

(14) Tamao, K.; Yamaguchi, S.; Ito, Y.; Matsuzaki, Y.; Yamabe, T.; Fukushima, M.; Moris, S. *Macromolecules* **1995**, *28*, 866.

(15) Ferraris, J. P.; Lambert, T. L. *J. Chem. Soc., Chem. Commun.* **1991**, 1268.

(16) Zotti, G.; Schiavon, G.; Berlin, A.; Fontana, G.; Pagani, G. *Macromolecules* **1994**, 27, 1983.

(17) Brédas, J. L. *J. Chem. Phys.* **1985**, *82*, 3808.

(18) Hong, S. Y.; Marynick, D. S. *Macromolecules* **1995**, *28*, 4991.

(19) Hong, S. Y.; Kwon, S. J.; Kim, S. C. *J. Chem. Phys.* **1995**, *103*, 1871.

(20) Lee, Y.-S.; Kertesz, M.; Elsenbaumer, R. L. *Chem. Mater.* **1990**, *2*, 526. Hoogmartens, I.; Adriaensens, P.; Vanderzande, D.; Gelan, J.; Quattrocchi, C.; Lazzaroni, R.; Brédas, J. L. *Macromolecules* **1992**, *25*, 7347.

(21) Hong, S. Y.; Marynick, D. S. *Macromolecules* **1992**, *25*, 4652.

(22) Hong, S. Y.; Song, J. M. *J. Phys. Chem. B* **1997**, *101*, 10249.

(23) Hong, S. Y.; Song, J. M. *J. Chem. Phys.* **1997**, *107*, 10607.

(24) Hong, S. Y.; Kwon, S. J.; Kim, S. C.; Marynick, D. S. *Synth. Met.* **1995**, *69*, 701.

10.1021/cm990547g CCC: $19.00

so far, a copolymer consisting of two thiophene rings and one benzo[1,2-*c*;3,4-*c*′]bis[1,2,5]thiadiazole ring in a unit cell is the only one which shows a $\pi-\pi^*$ absorption peak below 1.0 eV.[25]

To avoid the troublesome transition found in a nondegenerate system, we have recently performed a theoretical investigation on electronic properties of degenerate systems whose backbones are based on *trans*-polyacetylene (*t*-PA):polypentafulvalene (PFV **1**) and the related polymers.[26] PFV was predicted to possess a small band gap of 1.13 eV (corresponding to $\lambda_{\max} \approx 1100$ nm) by virtue of strong bonding interactions between the frontier orbitals of the *t*-PA backbone and the π^* orbital of the vinylene fragments fused onto the backbone. Substitution of methoxy groups at sites 5 and 5′ of PFV or cyano groups at sites 4 and 4′ was found to lower the band gap further. On the other hand, fusion of five-membered rings onto PFV was predicted not to affect the band gap appreciably, but to push energy levels of the frontier orbitals higher. To our knowledge, no oligomers or polymers of PFV systems have experimentally been prepared, although a variety of the substituted monomers have been prepared and are known to be stable toward air and light.[27−30]

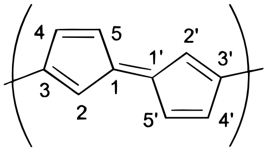

1

In this study, we performed quantum-chemical investigations on the electronic properties of PFV systems fused with six-membered rings, depicted in Figure 1, to search for very small band-gap polymers. We name the polymers as follows: poly(di-2-butenylene-pentafulvalene), P(1); poly(di-vinylenedioxy-pentafulvalene), P(2); poly(di-vinylenedithia-pentafulvalene), P(3); poly(dipyrazinopentafulvalene), P(4); and poly(di-ethylenedioxy-pentafulvalene), P(5). The fragments in P(1) to P(3) are different from that in P(4) in that the former fragments have two more π-type electrons than the latter. The ethylenedioxy fragment in P(5) was included since the fusion of the fragment has been known to reduce the band gap of polythiophene by about 0.5 eV without corrupting the planarity of the polymer chain.[31, 32]

Methodology

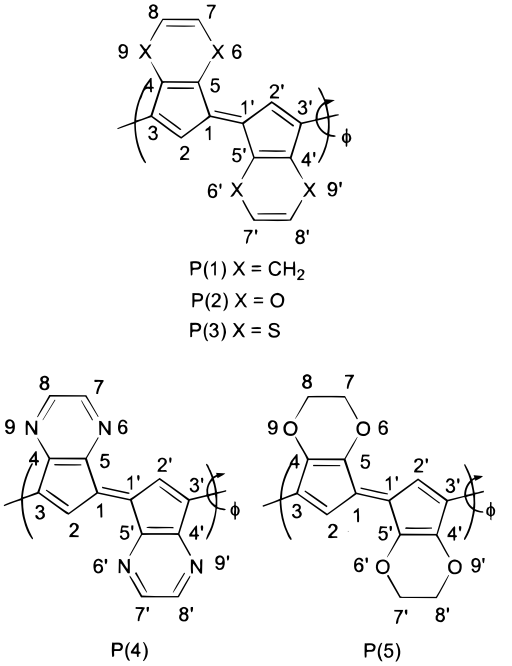

Figure 1. Polypentafulvalenes fused with six-membered-ring investigated in this study.

Quantum-chemical band calculations were performed to obtain ground-state structures of the polymers, as shown in Figure 1, at the Austin Model 1 (AM1) level, which is implemented by MOSOL,[33] the solid-state version of semiempirical methods. This version adopts the Born−von Kármán periodic boundary condition and Bloch functions for crystal calculations. The AM1 calculation is known to produce quite satisfactory conformational behaviors for a variety of conjugated molecules in comparison with ab initio and experimental data although the calculation yields low rotational barriers.[34] However, quantum-mechanical calculations for one polymer chain may not correctly produce the conformations for the condensed phase, since the calculation does not include interchain interactions. Packing of polymer chains would increase planarity of a polymer in the condensed phase. Therefore, to figure out the conformations of polymers in the condensed phase, examining a potential energy surface with respect to torsional angles is more informative than just locating the global minimum.

First, geometric parameters (bond lengths and bond angles) of the polymers were optimized for the planar conformation under a constraint of inversion symmetry. A small set of wave vectors and neighboring unit cells is used in the calculations to save the computational time. Six representative wave vectors (k) were chosen from 0 to π/a (a is the unit cell length) with regular intervals and the neighboring unit cells as far as the third nearest ones were involved in the lattice sum. It was observed in the previous calculation[26] for PFV that a large set of wave vectors (21 k points) and neighboring cells (6 unit cells on each side of the central unit) produced the same results as the small set we used in this study. Then, to examine conformational behaviors of the polymers, we took a unit cell twice as large as

---

(25) Kitamura, C.; Tanaka, S.; Yamashita, Y. *Chem. Mater.* **1996**, *8*, 570.

(26) Hong, S. Y.; Lee, K. W. *Chem. Mater.* **2000**, *12*, 155.

(27) Fallon, L.; Ammon, H. L.; West, R.; Rao, V. N. M. *Acta Crystallogr. B* **1974**, *30*, 2407. Kwistowski, P. T.; West, R. *J. Am. Chem. Soc.* **1966**, *88*, 4541. Ginsberg, A. E.; Paatz, R.; Korte, F. *Tetrahedron Lett.* **1962**, 779. Mark, V. *Tetrahedron Lett.* **1961**, 333.

(28) Prinzbach, H.; Sauter, H. *Angew. Chem., Int. Ed. Engl.* **1972**, *11*, 133.

(29) Brand, R.; Krimmer, H.-P.; Lindner, H.-J.; Sturm, V.; Hafner, K. *Tetrahedron Lett.* **1982**, *23*, 5131.

(30) Escher, v. A.; Neuenschwander, M.; Engel, P. *Helv. Chim. Acta* **1987**, *70*, 1623. Bergmann, E. D. *Chem. Rev.* **1968**, *68*, 41.

(31) Pei, Q.; Zuccarello, G.; Ahlskog, M.; Inganäs, O. *Polymer* **1994**, *35*, 1347.

(32) Fu, Y.; Cheng, H.; Elsenbaumer, R. L. *Chem. Mater.* **1997**, *9*, 1720.

(33) Dewar, M. J. S.; Zoebisch, E. G.; Healy, E. F.; Stewart, J. J. P. *J. Am. Chem. Soc.* **1985**, *107*, 3902. Stewart, J. J. P. *QCPE Bull.* **1985**, *5*, 62. Cui, C. X.; Kertesz, M. *J. Am. Chem. Soc.* **1989**, *111*, 4216.

(34) Fabian, W. M. F. *J. Comput. Chem.* **1988**, *9*, 369.

Table 1. Valence Shell Atomic Parameters Used in the Modified Extended Hückel Band Calculations

atom	*n*	*l*	IP (eV)	ζ (a.u.)	*n*	*l*	IP (eV)	ζ (a.u.)
H	1	0	13.60	1.300				
C	2	0	21.40	1.625	2	1	11.40	1.625
N	2	0	26.00	1.950	2	1	13.40	1.950
O	2	0	32.30	1.975	2	1	14.80	1.975
O[a]	2	0	32.30	2.275	2	1	14.80	2.275
S	3	0	20.0	2.117	3	1	13.30	2.117

[a] Parameters for oxygen in the ethylenedioxy fragment of P(5).

the one for the planar form, and constructed potential energy curves with respect to a torsional angle (ϕ) between the fulvalene units. Total energies of the twisted structures were calculated just by varying ϕ by 10°, from 0° to 90°, while the other geometric parameters are unvaried. If an energy minimum was found, the geometric parameters for the twisted structure were fully optimized to compare the energy with that for the planar conformation.

Electronic properties of the polymers were obtained by applying the AM1-optimized structures to a modified extended Hückel (MEH) method.[35] The MEH method adopts the off-diagonal elements into a new form, which has an additional distance-dependent empirical factor. This approach was parametrized to reproduce band gaps defined as the $\lambda_{\max}$ for the $\pi-\pi^*$ transition of conjugated polymers, and not the band edges as are often used to define the gaps experimentally. Typically, the band edge is about 0.5 eV lower than the peak value. This lowering coincides with estimated exciton binding energies[36] of conjugated polymers. In fact, photoluminescence measurements of poly(*p*-phenylene)[37] and polythiophene[38] demonstrated that photoexcitation occurs near a band edge of the absorption. Moreover, photoconductivity,[39] electroreflectance,[40] and electron energy loss spectroscopy[41] investigations of *t*-PA and polydiacetylenes revealed that the $\pi-\pi^*$ interband transitions occur at a higher energy by ~0.5 eV than the lowest exciton transitions. We believe that these experimental observations support our choice of a band gap of a conjugated polymer as a peak value of the absorption spectrum. The MEH method has been shown to yield reliable band gaps for a wide variety of π-conjugated polymers within errors less than 0.3 eV.[23,35,42] MEH parameters used in the calculations are listed in Table 1. The same Slater orbital exponents (ζ) for oxygen in P(5) are used as the ones in methoxy-substituted poly(*p*-phenylenevinylenes).[42]

Table 2. Optimized Geometric Parameters for the Planar Conformation of Polypentafulvalenes (PFVs) Fused with Six-Membered Rings in Figure 1 (Bond Lengths Are in Angstroms, and Bond Angles, in Degrees)

	PFV[a]	P(1)	P(2)	P(3)	P(4)	P(5)
R(1−2)	1.477	1.479	1.485	1.477	1.476	1.484
R(2−3)	1.373	1.374	1.377	1.373	1.373	1.376
R(3−4)	1.485	1.487	1.477	1.488	1.484	1.478
R(4−5)	1.361	1.373	1.373	1.375	1.462	1.376
R(5−6)		1.474	1.385	1.673	1.339	1.374
R(6−7)		1.487	1.402	1.676	1.357	1.440
R(7−8)		1.336	1.343	1.331	1.413	1.525
R(4−9)		1.474	1.380	1.670	1.339	1.371
R(8−9)		1.487	1.405	1.678	1.357	1.441
R(1−1′)	1.342	1.347	1.341	1.349	1.347	1.342
R(3′−3″)	1.426	1.434	1.424	1.435	1.431	1.424
θ(2−3−4)	108.3	107.1	107.0	107.2	108.1	107.0
θ(3−4−5)	108.9	109.1	109.3	109.0	107.5	109.3
θ(1−5−4)	108.6	109.0	109.3	109.0	107.6	109.1
θ(4−5−6)		123.6	124.3	126.9	122.1	124.6
θ(5−6−7)		112.3	111.2	105.3	115.2	110.6
θ(1′−1−5)	127.2	129.2	128.6	128.8	127.4	128.5
θ(3″−3′−4′)	123.6	125.7	124.7	125.5	124.0	124.8
δr[b]	0.098	0.099	0.100	0.097	0.099	0.099

[a] Data from ref 26. [b] Average value of the bond-length alternation, defined as $\delta r = |R(2-3) - R(1-2) + R(1-1') - R(1'-2') + R(2'-3') - R(3'-3'')|/3$.

Geometrical Structures

Optimized geometric parameters for the planar conformation of the polymers are summarized in Table 2 in comparison with those for PFV. In P(5), one C atom in the ethylene fragment is positioned above the polymeric plane and the other C atom below the plane so that hydrogen atoms in the fragment are staggered to avoid the repulsion between them. It is found that fusion of the six-membered rings on PFV slightly increases the bond length, R(4−5), between C4 and C5 atoms. This trend is more distinct in P(4), and R(4−5) becomes longer than R(7−8). It is also noteworthy in P(4) that all C−N bonds are similar in length. When six-membered rings containing vinylenedioxy or ethylenedioxy fragments are fused onto PFV, R(1−2) slightly increases and R(3−4) slightly decreases. On the other hand, upon fusion of the rings containing the other fragments, R(1−1′) and R(3′-3″), slightly increase to alleviate the large repulsion between the fulvalene units. However, the bond lengths along the *t*-PA-like chain do not significantly change and all the polymers accordingly possess bond-length alternations in the range of 0.097−0.100 Å, similar in value to those of PFV and *t*-PA.[26,43]

Conformational study reveals that among the polymers P(2) and P(5) would be of the planar conformation in their ground state although their potential curves are nearly flat up to $\phi \approx 20°$ within a energy difference of 0.5 kcal/mol of fulvalene units. In both P(2) and P(5), the closest atomic distance between oxygen and the hydrogen in the neighboring ring is estimated at 2.43 Å, which is smaller in value than the sum (2.6 Å) of van der Waals (vdW) radius of each atom.[44] Therefore, π conjugation along the polymeric chain is expected to be strong enough to overcome such a weak van der Waals repulsion. The strong tendency toward planarity has also been found in methoxy substituted poly(*p*-phenylenevinylenes).[42]

---

(35) Hong, S. Y.; Marynick, D. S. *J. Chem. Phys.* **1992**, *96*, 5497.

(36) Alvarado, S. F.; Seidler, P. F.; Lidzey, D. G.; Bradley, D. D. C. *Phys. Rev. Lett.* **1998**, *81*, 1082. Tasch, S.; Ekström, O.; Jost, T.; Scherf, U.; Leising, G. *Synth. Met.* **1997**, *85*, 1251. Mizes, H. A.; Conwell, E. M. *Synth. Met.* **1995**, *68*, 145.

(37) Leising, G.; Leitner, O.; Aldrian, F.; Kahlert, H. *Synth. Met.* **1987**, *17*, 635.

(38) Kaneto, K.; Yoshino, K. *Synth. Met.* **1989**, *28*, C287. Sauvajol, J. L.; Chenouni, D.; Hasoon, S.; Lere-Porte, J. P. *Synth. Met.* **1989**, *28*, C293. Shinar, J.; Vardeny, Z.; Ehrenfreund, E.; Brafman, O. *Synth. Met.* **1987**, *18*, 199. Vardeny, Z.; Ehrenfreund, E.; Shinar, J.; Wudl, F. *Phys. Rev. B* **1987**, *35*, 2498.

(39) Donovan, K. J.; Wilson, E. G. *J. Phys. C* **1979**, *12*, 4857. Yee, K. C.; Chance, R. R. *J. Polym. Sci. Polym. Phys.* **1978**, *16*, 431. Chance, R. R.; Baughman, R. H. *J. Chem. Phys.* **1976**, *64*, 3899.

(40) Sebastian, L.; Weiser, G. *J. Chem. Phys.* **1981**, *62*, 447.

(41) Ritsco, J. J.; Crecelius, G.; Fink, J. *Phys. Rev. B* **1983**, *27*, 4902. Ritsco, J. J.; Mele, E. J.; Heeger, A. J.; MacDiarmid, A. G.; Ozaki, M. *Phys. Rev. Lett.* **1980**, *44*, 1351.

(42) Hong, S. Y. *Bull. Korean Chem. Soc.* **1999**, *20*, 42.

(43) Hong, S. Y. *Bull. Korean Chem. Soc.* **1995**, *16*, 845.

(44) *Handbook of Chemistry and Physics*, 70th ed.; CRC Press Inc.: Boca Raton, FL, 1990.

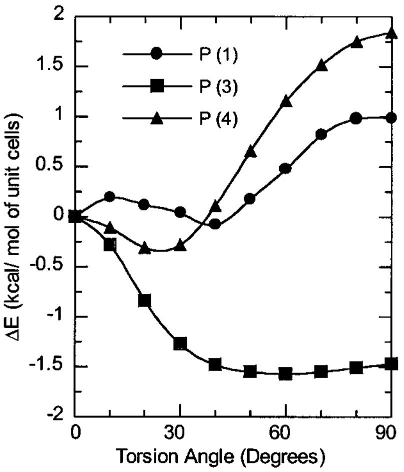

Figure 2. Torsional potential curves for P(1), P(3), and P(4).

As shown in Figure 2, two minima in the potential curve for P(1) appear at $\phi = 0°$ and 40°. At $\phi = 0°$, the closest distances between hydrogen bonded to C2 (C2′) and two hydrogen atoms in the methylene group of neighboring unit are only 2.11 Å, which are shorter than double the vdW radius (1.2 Å) for hydrogen. As the torsional angle increases up to 20°, one of the distances becomes shorter although the other becomes longer. Therefore, the potential energy slightly increases, and at a torsional angle of about 10° the energy starts to decrease. The full optimization reveals that the twisted conformation with an optimized torsional angle of 46.2° is only 0.4 kcal/mol of fulvalene units lower in energy than the planar conformation. The energy barrier when going from the twisted conformation to the planar one is estimated to be at most 0.6 kcal/mol of fulvalene units. In P(3), the large vdW radius (1.85 Å) of S requires a large torsional angle to avoid the severe steric repulsion between H bonded to C2 (C2′) and S in the neighboring ring. Figure 2 shows that the potential energy of P(3) decreases up to $\phi = 40°$ and becomes nearly flat. The potential energy curve for P(4) shows a minimum at $\phi \approx 25°$. The closest distance between H bonded to C2 (C2′) and N in the neighboring ring is 2.49 Å at $\phi = 0°$. At an optimized torsional angle of 26.7°, the distance becomes 2.69 Å, which is the same as the sum (2.7 Å) of vdW radii of H and N atoms, and the potential energy becomes lower by about 0.4 kcal/mol of fulvalene unit.

Electronic Structures

Table 3. Electronic Properties (in eV) for the Planar Conformation of Polypentafulvalenes (PFVs) Fused with Six-Membered Rings

	PFV[a]	P(1)	P(2)	P(3)	P(4)	P(5)
E_g[b]	1.13	1.11[e]	0.03	0.03[f]	1.16[g]	0.77
E_{HOMO}	−12.07	−11.95	−9.50	−10.18	−11.87	−11.30
E_{LUMO}	−10.94	−10.84	−9.46	−10.15	−10.71	−10.53
HVBW[c]	0.70	0.25	0.01	0.00	0.92	0.00
LCBW[d]	1.70	1.85	1.02	1.45	1.93	2.13

[a] Data from ref 26. [b] Band gap, defined as the λ_{max} for the $\pi-\pi^*$ transition. [c] HVBW = highest valence bandwidth. [d] LCBW = lowest conduction bandwidth. [e] At the optimized torsional angle of 46.2°, $E_g = 1.64$ eV. [f] At the optimized torsional angle of 73.2°, $E_g = 0.38$ eV. [g] At the optimized torsional angle of 26.7°, $E_g = 1.34$ eV.

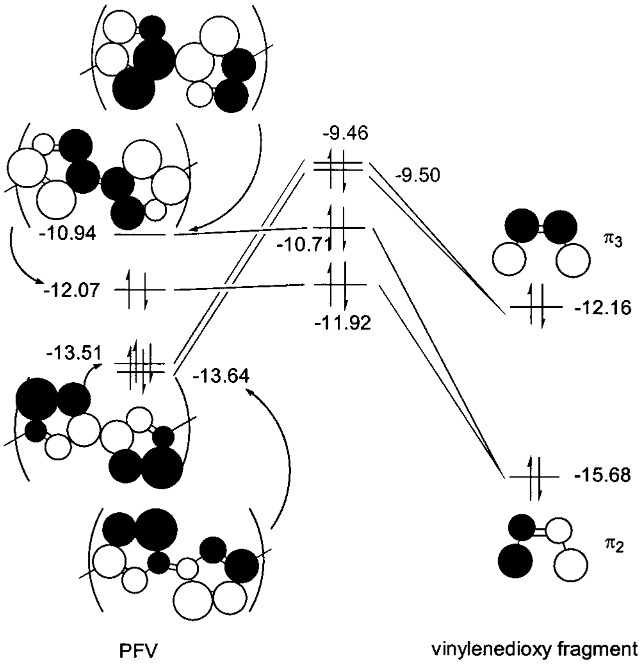

Figure 3. Molecular orbital correlation diagram for the interactions of vinylenedioxy fragments with PFV (energy in electronvolts).

The predicted electronic properties for the planar conformations of the polymers are compared with those for PFV in Table 3. Surprisingly, P(2) and (3) are predicted to possess nearly zero band gaps while the other polymers are estimated to possess band gaps close in value to that of PFV. Figure 3 shows the interactions of the vinylenedioxy fragments with PFV near the Fermi level. In the vinylenedioxy fragment, the π-type p orbitals of two terminal oxygen atoms possess coefficients of opposite signs in the π_2 orbital while they hold coefficients of the same sign in the π_3 orbital. Therefore, the π_2 orbital of the fragment interacts with the highest occupied molecular orbital (HOMO) and the lowest unoccupied MO (LUMO) of PFV. It is, however, estimated that these interactions are weak due to the large energy differences between the π_2 level and the frontier orbital levels, and that the latter levels are slightly pushed up by ~0.2 eV. On the other hand, the π_3 orbital level is so close to the energy levels of the HOMO−1 and the HOMO−2 orbitals of PFV that the interactions of the π_3 orbital are very strong with these orbitals. These strong interactions push up the energy levels far above the frontier orbital levels of PFV, resulting in the very low ionization potential and electron affinity of P(2). Because the HOMO−2 level of PFV is very close in energy to the HOMO−1 level, the band gap of P(2) turns out to be near zero despite the large bond-length alternation. No other symmetry-breaking geometrical distortion is expected to remove the near-degeneracy because the HOMO and LUMO of P(2) at the band edge of the Brillouin zone are localized mainly in the fused rings where no symmetry is imposed. In fact, Figure 4 shows the quite flat highest valence band (HVB) and the lowest conduction band (LCB) of P(2) at the Fermi level, reflecting the localization of the corresponding MOs. The same molecular orbital arguments as the ones made for P(2) still hold for the planar conformation of P(3). It is estimated even at a large ϕ of 73.2° that the band gap of twisted P(3) is only 0.38 eV. This is due to the nature of the flat HVB and LCB, which exhibits

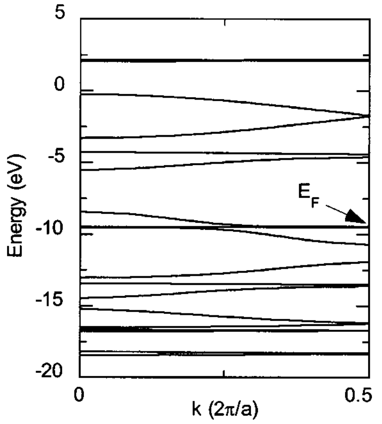

Figure 4. MEH-calculated π band structure of P(2).

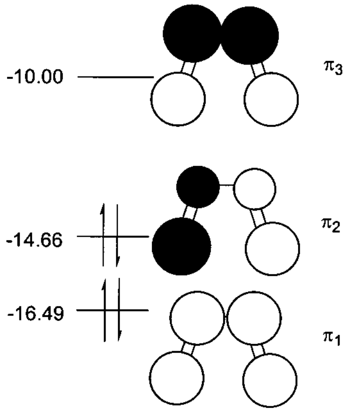

Figure 5. π Orbitals and energy levels (in electronvolts) of the ethanediylidenedinitrilo fragment.

small π overlaps along the *t*-PA-like backbone even at the planar conformation.

In the π_3 orbital of the 2-butenylene fragment in P(1), the atomic orbital coefficients of methylene C atoms are too small to produce large overlaps with π orbitals of PFV. As a result, the HOMO−1 and HOMO−2 orbitals of PFV weakly interact with the π_3 orbital, being destabilized by 0.7 eV. Furthermore, the interactions of frontier orbitals of PFV with the π_2 orbital of the fragment are much smaller because of the large energy differences between the corresponding energy levels of PFV and the fragment, leading to destabilization of the frontier orbitals only by 0.1 eV. Therefore, P(1) in the planar conformation is predicted to possess electronic properties similar to those of PFV.

As shown in Figure 5, the ethanediylidenedinitrilo fragment in P(4) has the same ordering of π orbitals with the vinylenedioxy fragment in P(2), but each orbital of the former is higher in energy than the corresponding orbital of the latter. Above all, the most distinctive difference between the fragments is that electrons do not occupy the π_3 energy level of the former fragment, but occupy the corresponding level of the latter. Therefore, in P(4) electrons do not occupy the energy levels which are produced through strong antibonding interactions between the π_3 orbital of the fragment and the HOMO−1 and the HOMO−2 orbitals of PFV. In fact, it is calculated that the LUMO+1 and the LUMO+2 orbitals of P(4) have molecular orbital characters similar to the HOMO and the LUMO of P(2), respectively. The frontier orbitals of P(4) result from the antibonding interactions between the π_2 orbital of the fragment and the frontier orbitals of PFV. Therefore, the band gap of P(4) is similar in value to that of PFV, but the oxidation potential and the electron affinity of the former are lower than those of the latter by 0.2 eV.

The LUMO of P(5) arises from the weak antibonding interaction between the LUMO of PFV and the π-type p orbitals of the terminal O atoms in the fragment, which have coefficients of opposite signs. On the other hand, the HOMO results from the strong antibonding interaction between the HOMO−1 orbital of PFV and the π-type O p orbitals where the coefficients are in the same sign. This implies that the interactions of the HOMO−1 and HOMO−2 orbitals of PFV with the π orbitals of the ethylenedioxy fragment are stronger than those found in P(1), but not as strong as those observed in the other polymers. As a result, the band gap of P(5) is estimated to be 0.77 eV, smaller than the gaps of P(1) and PFV, but much larger than the gaps of P(2) and P(3).

Conclusions

Fusion of the six-membered rings onto PFV is found not to induce a notable change in bond-length alternation along the *t*-PA-like backbone of PFV, but to significantly affect the planarity of the backbone except the cases of P(2) and P(5) which contain oxygen atoms in the rings. Conformational investigation, however, reveals that the energy differences between the planar and the twisted conformations of P(1) and P(4) are small and that the heights of the barriers between these conformations are also small. Therefore, in the con-

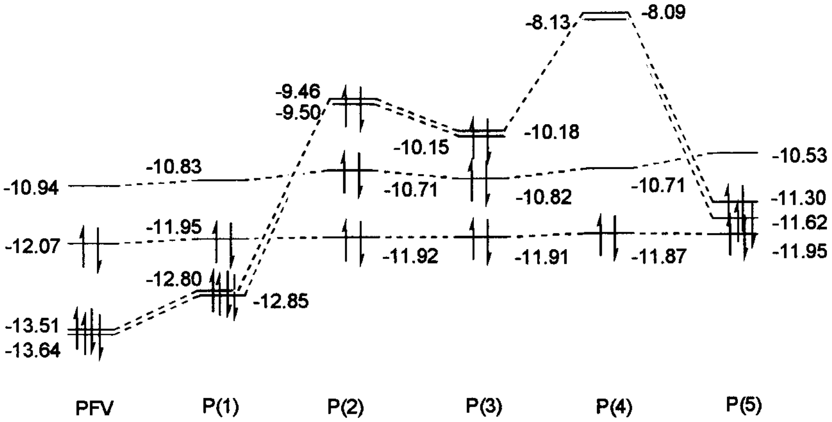

Figure 6. Variation of orbital energy levels (in electronvolts) of the PFV systems near Fermi level.

densed phase, P(1) and P(4) may also be of the planar conformation.

It is found that there are two different types of π interactions near the Fermi levels of the fused PFV systems. One of them is interactions between the frontier orbitals of PFV backbone and the π_2 orbital of a fragment in a fused ring, and the other between the HOMO−1 and HOMO−2 orbitals of the backbone and the π_3 orbital of the fragment. The former is very weak because of large energy differences between the corresponding orbital levels, pushing up the frontier orbital energy levels of PFV by only 0.1−0.2 eV. On the other hand, the latter type is dependent on the type of a fragment. Illustrated in Figure 6 is the variation of each energy level near the Fermi levels with the fragments. When π-overlaps between the HOMO−1 and HOMO−2 orbitals of PFV and the π_3 orbital of a fragment are large, the corresponding energy levels of PFV are pushed up above the frontier orbital energy levels of PFV as found in P(2) to P(4). Since the former two levels are nearly degenerate, P(2) and P(3) would possess almost zero band gaps. Note that the corresponding levels of P(4) are not occupied by electrons since each N atom in the ethanediylidenedinitrilo fragment possesses only one π electron. When the π overlaps are small, those energy levels are located below the HOMO of PFV as in P(1) or between the LUMO and the HOMO as in P(5). Therefore, it is estimated that the band gap of P(1) is similar in value to that of PFV while the gap of P(5) is slightly smaller.

Acknowledgment. The author acknowledges the financial support of Korea Research Foundation made in the program (1997-001-D00265) of 1997.

CM990547G